The necessary emergence of structural complexity in self-replicating RNA populations

Carlos G. Oliver[1], Vladimir Reinharz[1,2], Jérôme Waldispühl[1,*]

[1] School of Computer Science, McGill University, Montreal, Canada

[2] Center for Soft and Living Matter, Institute for Basic Science, Ulsan, South Korea

January 14, 2019

Abstract

The RNA world hypothesis relies on the ability of ribonucleic acids to replicate and spontaneously acquire complex structures capable of supporting essential biological functions. Multiple sophisticated evolutionary models have been proposed for their emergence, but they often assume specific conditions. In this work we explore a simple and parsimonious scenario describing the emergence of complex molecular structures at the early stages of life. We show that at specific GC-content regimes, an undirected replication model is sufficient to explain the apparition of multi-branched RNA secondary structures – a structural signature of many essential ribozymes. We ran a large scale computational study to map energetically stable structures on complete mutational networks of 50-nucleotide-long RNA sequences. Our results reveal that the sequence landscape with stable structures is enriched with multi-branched structures at a length scale coinciding with the appearance of complex structures in RNA databases. A random replication mechanism preserving a 50% GC-content may suffices to explain a natural enrichment of stable complex structures in populations of functional RNAs. By contrast, an evolutionary mechanism eliciting the most stable folds at each generation appears to help reaching multi-branched structures at highest GC content.

*To whom correspondence should be addressed. Tel: +1 514-398-5018; Email: `jeromew@cs.mcgill.ca`

1 Introduction

RNA are versatile molecules that can virtually fulfill all fundamental needs and functions of the living, from storing information to catalyzing chemical reactions and regulating gene expression. The RNA world hypothesis [1, 2] builds upon this observation to describe a scenario of the emergence of life based on RNAs. Despite criticisms [3–5], recent studies presented plausible paths towards an early assembly of RNA molecules has contributed to strengthening this hypothesis [6–10]. Yet, the emergence of nucleic acids is only one part of this problem. We also need to elucidate the mechanisms that enabled the discovery of functional molecules and the transmission of genetic information [11].

Many non-coding RNAs acquire functions through structures. Classically, we describe these structures at two levels of abstraction. The secondary structure encompasses the Watson-Crick and Wobble base pairs, while the tertiary structure describes the 3D coordinates of all atoms. Noticeably, RNA secondary structures are more conserved than sequences and thus provide a reliable signature of RNA function [12]. Moreover, many essential molecular functions are supported by nucleic acids with complex shapes often characterized by the occurrence of a k-way junction (a loop connecting three or more stem-like regions also known as multi-loop; See **Fig. 1c**) in their secondary structure (e.g. 5s rRNA, tRNA, hammerhead ribozyme). A theory describing how RNA populations evolve to "discover" these functional multi-branched secondary structures is therefore an important step toward a validation of the RNA world hypothesis [13].

Since the first analysis of RNA neutral networks (i.e. networks of RNA sequences with identical structures) [14], computer simulations are the method of choice for characterizing the evolutionary landscape and population dynamics of structured RNA molecules. Indeed, secondary structures can be reliably predicted from sequence data only [15], allowing fast and accurate prediction of phenotypes (i.e. secondary structure) from genotypes (i.e. sequence).

A large body of literature has been dedicated to the computational analysis of RNA sequence-structure maps (i.e. genotype-phenotype maps) and properties of RNA populations evolving under natural selection. In a seminal series of papers P. Schuster and co-workers set up the basis of a theoretical framework to study the evolutionary landscape of RNA molecules, and used it to reveal intricate properties of networks of sequences with the same structure (a.k.a. neutral networks) [14,

16–20]. This work inspired numerous computational studies that refined our understanding of neutral models [21–25], as well as kinetics of populations of evolving nucleic acids [26–28].

In this paper, we perform computer simulations to study the evolutionary mechanisms that enabled the emergence of multi-branched secondary structures. This feature turns out to be relatively common even for short RNAs. An analysis of the consensus secondary structures available in the Rfam database reveals that multi-loops can be found in approximately 10% of RNA families whose average size of sequences ranges from 50 to 100 nucleotides (See **Fig. 1a**). This observation contrasts with earlier studies that revealed that the vast majority of predicted minimum free energy (MFE) secondary structures obtained from a uniform sampling of shorter RNA sequences (i.e. 35 nt.) are stem-like structures (i.e. no multi-loop) [29], which render a spontaneous emergence of complex structures (i.e. secondary structures without multi-loop) unlikely on such short sequences.

Nonetheless, computational studies of RNA sequence-structure maps showed that neutral networks percolate the whole sequence landscape [30, 31]. Even though this property undeniably augments the accessibility of target structures, the size and connectivity of neutral networks also decreases drastically with the complexity of structures.

In the most commonly accepted scenarios, the establishment of a stable, autonomous, and functional self-reproductive molecular system subject to natural selection, relies on the presence of polymerases [13]. Such molecules are long (200 nt.) and thus unlikely to be discovered randomly. Instead, it has been suggested that evolution proceeded by stages [32]. Polymerases were assembled from smaller monomers ($\sim$50 nt.) that are more likely to emerge from prebiotic chemistry [33, 34]. At this point, and not before, parallel natural selection processes of specific functional structures could be triggered.

Interestingly, *in vitro* experiments revealed the extreme versatility of random nucleic acids [35–38], and suggested that essential RNA molecules such as the hammerhead ribozyme could have multiple origins [39]. All together, these observations reinforce the plausibility of a spontaneous emergence of multiple functional sub-units. But they also question us about the likelihood of such events and the existence of intrinsic forces promoting these phenomena.

Various theoretical models have been proposed to highlight mechanisms that may have favoured the birth and growth of structural complexity from replications of small monomers. Computational studies have been of tremendous help to explore various scenarios. In particular, numerical simula-

tions enabled us to study the effects of polymerization on mineral surfaces [40, 41] or the importance of spatial diffusion [42]. Noticeably, the majority of these scenarios are proposing a development of RNA structural complexity outside a cellular barrier. But this assumption results in major challenges. The first of them is to explain how a system that evolved and adapted in an exposed milieu would transition to a membrane-protected environment. In particular, the presence of a membrane would radically change the tradeoff between stability and complexity of RNA structures. Indeed, stable folds often lack the complexity necessary to support novel functions but are more resilient to harsh pre-cellular environments [43].

In this work, we aim to characterize the structural repertoire accessible by self-replicating RNA populations. This scenario is compatible with the hypothesis of an early development of membranes [11, 44–46] and does not require invoking hybridization on surfaces. Importantly, we exclude directed evolution scenarios characterized by a progressive adaptations to a phenotype (e.g self-replication with errors minimizing the distance of MFE structures to a target structure [47]). Instead, we rely on intrinsic forces (i.e. increasing secondary structure stability) for driving the evolutionary process and study the impact of GC-content bias.

We apply customized algorithms to map secondary structures on all mutant sequences with 50 nucleotides [48, 49]. This approach considerably expands the scope and significance of comprehensive RNA evolutionary studies that were previously limited to sequences with less than 20 nucleotides [18, 50], or restricted to explore a small fraction of the sequence landscape of sequences [25, 29]. Our simulations reveal that based on the strength of the selective pressure applied on the self-replicating population, different GC content biases facilitate the emergence of complex secondary structures with k-way junctions. In the absence of selective pressure, low to medium GC contents (0.3-0.5) may suffice to explain the distribution of multi-loop structures observed in databases. By contrast, high GC contents help populations eliciting sequences with stable folds to discover structure with k-way junctions. These results provide valuable insights into previous contributions studying GC content biases in stability-flexibility tradeoffs [51], prebiotic nucleotide distributions [52, 53] and the accessibility of complex phenotypes [29].

2 Results

2.1 Our approach

We apply complementary techniques to explore the RNA mutation landscape and characterize the structures accessible from an initial pool of random sequences under distinct evolutionary scenarios (See **Fig. 2**). Importantly, our analysis explicitly models GC content bias to understand the effect of potential nucleotide scarcity in prebiotic conditions [52, 53].

Our first algorithm `RNAmutants` (see Sec. 4.2) enumerates all mutant sequences and samples the ones with the *globally* lowest folding energy [48]. It enables us to identify the most stable structures accessible through random replication processes without selective pressure (i.e. the discovery hypothesis). Noticeably, `RNAmutants` sorts the sequences by the number of mutations separating them from the initial population.

An important element of this work is the interpretation of `RNAmutants` curves where the x-axis shows the number of mutations (e.g. **Fig. 3a**). When this number of mutations is null or very low, the data represents the values we expect from uniformly sequences sampled. By contrast, large numbers of mutations are associated with an increased preference for mutants with stable folds and a loss of sequence specificity. The largest hamming neighbourhoods (See **Fig. S6**) are therefore the ones with strongest thermodynamical pressure.

Our second algorithm `mateRNAl` has been developed for this study. It simulates the evolution of a population of RNA sequences that preferentially selects the most stable structures under GC content bias. We also developed variants of this algorithm enabling us to study the antagonistic effect of a negative selection pressure against the most stable structures.

We study the evolutionary landscape of RNA sequences of length 50 preserving GC contents varying between 0.1 and 0.9 (1 being full G or C sequences). The size of molecules is of particular interest as 50 nucleotides appears to be the upper limit for non-enzymatic self-replicating processes [13], but also because multi-branched structures occur only on RNAs with sizes above 40 (See **Fig. 1**). It also turns out to the be minimal known size for a ribozyme [54].

2.2 Energy landscape of RNA mutational networks

We start by characterizing the distribution of folding energies of stable structures accessible from random seeds in the mutational landscape using `RNAmutants`. Our simulations show that, initially, increasing mutational distances from random seeds results in more stable structures at all GC content regimes (See solid lines in **Fig. 3a**). We observe that the folding energies of the samples represent at least 80% of the global minimum energy attainable over all k mutations within less than 10 mutations from the seed (see **Fig. S2**). This suggests that over short evolutionary periods, mutations can play an important stabilizing role as stable structures are likely to be found near the seed.

By contrast, at larger mutational distances (i.e. 15 mutations and above) we notice an increase in the ensemble energy for all GC content regimes. This behaviour is likely due to the exponential growth in sequence space that accompanies higher mutational distances, which results in a more uniform sampling of the ensemble. In this case, less stable sequences outnumber lower energy sequences with high Boltzmann weights (See **Fig. S1**).

As expected, we observe that the nucleotide content is an important factor in determining the stability of achieved sequence-structure pairs across mutational networks. The accessible sampled energies are strongly constrained by the allowed GC content of sequences in all GC content regimes, whereby higher GC contents favor the sampling of more stable states. However, despite these constraints, all mutational ensembles effectively produce more stable states than the initial state.

Next, we characterize the diversity of structures sampled by `RNAmutants`. First, we calculate the number of unique structures found in each mutant neighbourhood. **Fig. 3b** shows two distinct regimes. At low to intermediate GC contents (≤ 0.5), the immediate neighbourhood (≤ 10 mutations) of seed sequences is dominated by few stable structures, after what the percentage of unique structures suddenly increases. This sudden change of regime accompanies the increase of the average folding energies observed in **Fig. 3a**. By contrast, at higher GC contents (≥ 0.7) the structural diversity increases only at very large mutational distances (≥ 40), when the footprint from the seed is almost fully lost.

We also explore the repertoire of secondary structure elements represented in the low energy mutational neighbourhoods. **Fig. S4** and **4a** show the percentage of secondary structures with an

internal loop or multi-loop. Although these structural elements are relatively frequent in random sequences (i.e. seeds), they are also not very stable (**Fig. 3a**). When the mutational distance increases, mutations tend to create stable stem-loop structures and erase irregularities in the original phenotypes. Although, after this stabilization phase, the fraction of internal and multi-branched loops rises again explaining the structural diversity discussed above.

In this work, we focus on the occurrence of multi-branched secondary structures because this motif is often found in functional RNAs such as the hammerhead ribozyme. While previous studies of short randomly sampled RNA sequences (< 35 nt.) have shown that simple hairpin structures dominate the low-energy structural landscape, we find that for longer molecules (i.e. 50 nt.) this landscape is enriched with complex multi-branched structures. This finding is in good qualitative agreement with databases of evolved structures where multi-loop structures emerge in families slightly under 50 nucleotides long (**Fig. 1a**).

Across all runs, we sampled a total of 9419 sequences containing a multi-loop (no more than 1 multi-loop per structure was ever observed as is to be expected for such length scales). Interestingly, we find that unlike internal loops, multi-loops occur under very specific conditions in our sampling. We identify a clear surge of multi-loops frequency at distances at a mutational distance of ~ 35 (See **Fig. 4a**), with a mean GC content of ~ 0.45 (See **Fig. 4c**). Furthermore, their energy distribution is tightly centered around $\sim -15\,\mathrm{kcal\,mol^{-1}}$ (See **Fig. 4d**). These values are remarkably close to the those of multi-branched structures of similar lengths observed in the Rfam database (See **Fig. 1b**). In particular, the latter shows a clear bias toward medium GC contents as we identified 148 Rfam families with multi-loops with a GC content of 0.5 (among all Rfam families with sequences having at most 200 nucleotides), but only 80 with a GC content 0.3 and 40 with a GC content of 0.7. This serves as further evidence that GC content is an important determinant of the evolution of structural complexity. It also appears that these features are a general property of the distribution of multi-loops in the mutational landscape given the sequence entropy of the set of sequences containing multi-loops is quite high (0.945 out of 1). This indicates that the observed properties are likely a feature of the GC content bias and not due to over-representation by isolated groups of similar sequences. Further analysis carried out in Section 2.3 suggests that this enrichment of complex structures is not simply an artifact of larger Hamming neighbourhoods that accompanies deeper mutational explorations.

We also note a smaller peak of multi-loop occurences closer to the seed sequences (~ 6 mutations) for higher GC contents around 0.7. Interestingly, with folding energies ranging from -25 to $-40\,\mathrm{kcal\,mol^{-1}}$, these multi-branched structures are significantly more stable than those present in the main peak (See **Fig. 4b**). This is also in agreement with the energies observed in the Rfam database for structures within this range of GC content values (See **Fig. 1b**).

Observation 1

- Low and intermediate GC contents (≤ 0.5) promote structural diversity.
- Internal and multi-branched loops are relatively frequent in the low-energy landscape.
- The frequency of stable multi-branched loops in the low-energy landscape is in good qualitative agreement with the Rfam distribution.

2.3 Random replication *without* selection

In the previous section, we observed that the low-energy structural landscape is enriched with multi-loop architectures at specific GC contents. We must next determine under which conditions a self-replicating population can reach this reservoir. Our first scenario aims to study the behaviour and outcome of random replication process *without natural selection*. Here, we consider a simple model in which RNA molecules are duplicated with a small error rate, but preserving the GC content [55]. In our simulations, we use an error rate of 0.02 (probability of introducing a point mutation) to allow immediate comparison of the number of elapsed generations, and identical transitions and transversions rates. Under these assumptions, we can directly compute the *expected* number of mutations in sequences at the ith generation (see Methods). **Fig. S5** shows the results of this calculation for GC content biases varying from 0.1 to 0.9. Noticeably, our data reveals that after a short initialization phase (i.e. after ~ 50 generations), sequences with a GC content of 0.5 have on average slightly more than 35 mutations. This observation is in good adequacy with the peak of multi-branched structures identified in **Fig. 4a** and **Fig. 4c**. This combination of events suggests that the population is randomly exploring the sequence landscape and gets fixed once stable structures are discovered. Indeed, the mutation distance where multi-loops are observed coincides with the largest mutational neighbourhood (See **Fig. S6**), thus where the sequence specificity pressure is minimal. We conclude that a simple undirected replication mechanism could explain an

enrichment of RNA populations with stable multi-branched structures.

To complete this analysis and assess the different structural compositions between the uniform and low-energy landscapes, we sample sequences at each mutational neighbourhood uniformly at random and compute their minimum free energy (MFE) value and secondary structure. We compare in **Fig. 5** the average MFE and frequency of multi-loops in MFE structures between the uniform ("Random") samples and sequences sampled from the `RNAmutants` low-energy ensemble. Importantly, we report apart the statistics for sequences with or without multi-loops.

Unsurprisingly, the accumulation of mutations does not impact the results in random populations. First, we note that although multi-branched structures are relatively frequent in random populations (in average between 1 and 10%), they also have higher folding energies than sequences in the low-energy landscape. Higher GC contents tend to increase these trends. This data supports previous observations made on shorter sequences showing that multi-branched structures are rare and relatively unstable in random pools of sequences [29].

By contrast, `RNAmutants` samples exhibit a different pattern. While multi-branched structures are rare in random populations (i.e. no mutations), their frequency increases with the number of mutations (i.e. increased preference toward stable structures). Interestingly, the frequency of stable multi-branched structures almost matches those obtained with random sequences at GC contents between 0.3 and 0.5 and mutational distances from 30 and 40 (second row in the third and fourth columns of **Fig. 5**).

The analysis of folding energies reveals another interesting phenomenon. While the average energies of multi-branched structures remains steady at all mutational distances, this is not the case of other structures with simpler architectures (first row of **Fig. 5**). Lower GC content regimes from 0.3 to 0.5 are characterized by a clear increase of average energies at mutational distances over 20 (i.e. MFE structures are less stable), which is not observed at higher GC contents. We conclude from these observations that the relative weight of multi-branched structures in the low energy ensemble (i.e. `RNAmutants`) increases due to a better (collective) resilience of this architecture to point-wise mutations and/or a more uniform distribution in the sequence landscape. In turn, it increases their density in the large/distant mutational neighbourhoods. Moreover, it is worth noting that the values of the folding energies at these GC regimes are also close to those observed in Rfam.

Eventually, we also distinguish a secondary peak of occurrences of multi-branched structures in the vicinity of the seeds (i.e. 5-10 mutations) at higher GC regimes (0.7). By contrast, this higher density appears to result from mutants folding with marginally lower energies. It suggests the presence of mutants with improved fitness to the structures of the seeds rather than a global enrichment of multi-branched structures in these neighbourhoods. We discuss this phenomenon in the next sub-section.

Observation 2

- Multi-branched structures are relatively common but unstable in random populations.
- At intermediate GC contents ($0.3 - 0.5$), multi-branched loops are frequent among the stablest structures.
- The folding energies of stable multi-loop is similar to those observed in databases.

2.4 Random replication with selection for stable structures

Our `RNAmutants` and random replication simulations suggest that mutational networks contain reservoirs of complex structures accessible by undirected replication mechanisms. At this point, our main question is to determine if a natural selection process, independent of a particular target, could help reaching these regions.

To address this question we build an evolutionary algorithm named `mateRNAl`, where the fitness is proportional to the folding energies of the molecules. Intuitively, `mateRNAl` simulates the behaviour of a population of RNAs selecting at each generation the most efficient sequences (i.e. most stable) regardless of the structures adopted to carry functions (See **Methods 4.1**). These selected structures are therefore by-products of intrinsic adaptive forces.

We start all simulations from random populations of size 1000 and sequences of length 50, and performed 50 independent simulations for each GC content and varying mutation rates. Importantly, we also vary the strength of the selective pressure applied on the population (i.e. the β in Eq. 1). All simulations were run for 1000 generations.

We show the frequency and folding energy of multi-branched structures observed during our simulations with `mateRNAl` in **Fig. 6**. Here, a higher selective pressure (i.e. larger values of β) and GC content reduces the frequency of multi-loops but increases the folding energy. Interestingly,

a transition occurs when the value of β shift from 0.01 to 0.05. By contrast, higher GC contents increase both the frequency of multi-loops and folding energies. Yet, variations of the selective pressure result in more variance of the folding energy.

In our simulations, only highest GC contents ($\geq$ 0.7) produce populations with multi-loop frequencies comparable to those observed in databases. It follows that the `mateRNAl` evolutionary scenario does not seem fit to explain how to reach multi-branched sequences with low to intermediate GC content (0.3−0.5). However, as noted earlier, there is a second pool of multi-branched structures at higher GC content ($\geq$ 0.7) that are characterized by their proximity to the seed (See **Fig. 4a**) and lower folding energies (See **Fig. 4b**). Under our assumption, the `mateRNAl` scenario appears to be a legitimate candidate to explain how these structures are reached.

We find that `mateRNAl` populations are able to quickly find low energy multi-branched structures (less $\sim$ 12 mutations from the initial populations; See **Fig. 6**), with higher GC content regimes leading to more stable structures. Multi-branched structures are mostly found near the seeds ($\leq$ 20 mutations) and rather in earlier generations.

We also note an interesting dichotomy between populations at 0.7 and 0.9 GC ratios. While the frequency of multi-loops reached by populations at 0.7 roughly matches the one computed by `RNAmutants` (See **Fig. 4a**), it is not the case for higher GC contents. Indeed, the `mateRNAl` simulations find a significant number of multi-loops not sampled by `RNAmutants`. The folding energies of these structure appears to be similar to the ones found in Rfam (See **Fig. 1b**).

All together, these observations suggests that a selective pressure on stable structures might help finding stable multi-branched architectures at the highest GC contents (i.e. 0.9) that are otherwise eclipsed by the vast number of stable single stem structures. At 0.7 though this selection mechanism could still be used to accelerate and promote the discovery of these complex structures uniformly distributed in the sequence landscape.

Observation 3

- Multi-loops emerge only in populations with highest GC contents ($\geq$ 0.7).
- Highest GC contents help to quickly reach multi-loops in the vicinity of the seeds.
- A selection pressure toward stable structure promote the discovery of rare stable multi-branched structures at 0.9.

3 Discussion

We provided evidence that in the absence of selective pressure, the structure of the mutational landscape could have helped to promote the emergence of an RNA-based form of life. To support our hypothesis, we built a comprehensive representation of the mutational landscape of RNA molecules, and investigated scenarios based on distinct hypotheses.

Our results support parsimonious evolutionary scenarios based on undirected molecular self-replications with occasional mutations. In these simple models, the GC content appears as a key feature in determining the probability of discovering stable multi-branched secondary structures. Our study reveals two distinct phenomena. At low to intermediate GC contents ($0.3 - 0.5$) the distribution of multi-loops in a self-replicating population eliciting sequences with the most stable structures resembles the one observed in RNA databases. This observation suggests that an evolutionary scenario in which sequences are replicated without selection but where the most stable structures are selected upon their discovery is sufficient to explain the structural complexity needed for the emergence of life at the molecular level.

By contrast, at higher GC contents (≥ 0.7) the presence of multi-branched structures appears to require the help of a selective pressure to reach these complex phenotypes. In this work, we simulate self-replicating RNA populations selecting sequences with the most stable structures at each generation. Then, we show that this mechanism enables a quick discovery of multi-loops in the vicinity of random sequences at GC content regimes at or above 0.7. This finding is in agreement with previous theoretical studies that showed that neutral networks percolate the whole sequence landscape [30, 31]. It also suggests a different origin for multi-branched structures at high GC content. In such scenario, a population of molecule would progressively improve the functional efficiency of the molecules by improving their stability.

The preservation of intermediate GC content values appeared to us as a reasonable assumption, which could reflect the availability of various nucleotides in the prebiotic milieu. This nucleotide composition bias can be interpreted as an intrinsic force that favoured the emergence of life. It also offers novel insights into fundamental properties of the genetic alphabet [53]. Incidentally, these observations suggest further investigations into the role of more complex nucleotide distributions [56].

It is worth noting that our scenario remain compatible with further selection mechanisms that

may come into play once a functional and stable architecture is identified to rapidly improve active sites [25, 57]. Eventually, our results could also be used to put in perspective earlier findings suggesting that natural selection is not required to explain pattern composition in rRNAs [58].

Our analysis completes recent studies that aimed to characterize fundamental properties of genotype-phenotype maps [59, 60], and showed that their structure may contribute to the emergence of functional molecules [25]. Whereas previous studies focused on characterizing the static genotype-phenotype map of random sequences, we show that the map of stable mutants arising from random seeds favours the discovery of complex structures. It also emphasizes the relevance of theoretical models based on a thermodynamical view of prebiotic evolution [61].

The size of the RNA sequences considered in this study has been fixed at 50 nucleotides. This length appears to be the current upper limit for non-enzymatic synthesis [62], and therefore maximizes the expressivity of our evolutionary scenario. Variations of the sizes of populations or lengths of RNA sequences resulting from indels could be eventually considered with the implementation of dedicated algorithms [63]. Although, if these variations remain modest, we do not expect any major impact on our conclusions.

The error rates considered in this study were chosen to match values used in previous related works (e.g [64]). This choice is also corroborated by recent experiments suggesting that early life scenarios could sustain high error rates [65]. Nevertheless, lower mutation rates would only increase the number of generations needed to reach the asymptotic behaviour (See **Fig. S5**), and thus would not affect our results.

Finally, we emphasize that our results do not exclude the use of more advanced evolutionary mechanisms [40–42, 66]. Instead, they provide additional evidence supporting an RNA-based scenario for the origin of life, and can serve as a solid basis for further investigations of more sophisticated models.

4 Materials and Methods

4.1 Evolutionary Algorithm (`mateRNAl`)

4.1.1 Initial Population

Here we describe an evolutionary algorithm (EA) for energy-based selection with GC content bias. The algorithm is implemented in Python and is freely available at `http://jwgitlab.cs.mcgill.ca/cgoliver/maternal.git`.

We first define a population at a generation t as a set P_t of sequence-structure pairs. We denote a sequence-structure pair as (ω, s) such that s is the minimum free energy structure on sequence ω as computed by the software `RNAfold` version 2.1.9 [15]. Each sequence is formed as a string from the alphabet $\mathbb{B} := \{A, U, C, G\}$. For all experiments we work with constant population size of $|P_t| = 1000 \quad \forall t$, and constant sequence length $\texttt{len}(s_i) = 50 \quad \forall s_i \in P_t$. We then apply principles of natural selection under Wright-Fisher sampling to iteratively obtain P_{t+1} from P_t for the desired number of generations in the simulation.

Sequences in the initial population, i.e. generation $t = 0$, are generated by sampling sequences of the appropriate length uniformly at random from the alphabet $\mathbb{B}$.

4.1.2 Fitness Function

In order to obtain subsequent generations, we iterate through P_t and sample 1000 sequences with replacement according to their relative fitness in the population. Selected sequences generate one offspring that is added to the next generation's population P_{t+1}. Because we are sampling with replacement, higher fitness sequences on average contribute more offspring than lower fitness sequences. The relative fitness, or reproduction probability of a sequence ω is defined as the probability $F(\omega, s)$ that ω will undergo replication and contribute one offspring to generation $t+1$. In previous studies, $F(\omega_i, s_i)$ has been typically defined as a function of the base pair distance between the MFE structure of ω and a given target structure. However, in our model, this function is proportional to the free energy of the sequence-structure pair, $E(\omega, s)$ as computed by `RNAfold`.

$$F(\omega, s) = N^{-1} e^{\frac{-\beta E(\omega, s)}{RT}} \tag{1}$$

The exponential term is also known as the Boltzmann weight of a sequence-structure pair. N is a normalization factor obtained by summing over all other sequence-structure pairs in the population as $N = \sum_{\omega',s' \in S_t} \exp[\frac{-\beta E(\omega',s')}{RT}]$. This normalization enforces that reproduction probability of a sequence-structure pair is weighted against the Boltzmann weight of the entire population. β is the selection strength coefficient. Higher values of β result in stronger selection for stability and vice versa. $R = 0.000\,198\,71$ kcal mol^{-1} K^{-1} and $T = 310.15K$ are the Boltzmann constant and standard temperature respectively.

When a sequence is selected for replication, the child sequence is formed by copying each nucleotide of the parent RNA with an error rate of μ known as the mutation rate. μ defines the probability of incorrectly copying a nucleotide and instead randomly sampling one of the other 3 bases in $\mathbb{B}$.

4.1.3 Controlling population GC content

There are two obstacles to maintaining evolving populations within the desired GC content range of ± 0.1. First, an initial population of random sequences sampled uniformly from the full alphabet naturally tends converge to a GC content of 0.5. To avoid this, we sample from the alphabet with probability of sampling GC and AU equal to the desired GC content. This way our initial population has the desired nucleotide distribution. Second, when running the simulation, random mutations are able to move replicating sequences outside of the desired range, especially at extremes of mutation rate and GC content. To avoid this drift, at the selection stage, we do not select mutations that would take the sequence outside of this range. Instead, if a mutation takes a replicating sequence outside the GC range, we simply repeat the mutation process on the sequence until the child sequence has the appropriate GC content (See **Alg. 1**). Given that populations are initialized in the appropriate GC range, we are likely to find valid mutants relatively quickly and always avoid drifting away from the target GC.

```
input  : parentSeq, targetGC
output: childSeq
childSeq ← mutate(parentSequence)
while computeGC(childSequence) not in targetGC ± 0.1 do
  | childSeq ← mutate(parentSeq)
end
return childSeq
```

Algorithm 1: GC content maintaining replication

4.2 RNAmutants

The evolutionary algorithm is similar to a local search. At every time step new sequences are close to the previous population and in particular to the elements with higher *fitness*.

In contrast RNAmutants [48] can sample pairs of sequence-structure (ω, s) such that (1) the sequence is a k-mutant from a given seed ω_0—for any k—and (2) the probability of seeing the pair is proportional to its *fitness* compared to all pairs (ω', s') where w' is also an k-mutant of ω_0.

In addition RNAmutants provides an unbiased control of the samples GC content allowing direct comparisons with mateRNAl.

We note that although the structure sampled is not in general the MFE replacing them by it does not significantly change the results, as shown in Fig. **??**. Therefore we replace the sampled structure with the MFE to simplify the study.

For each GC content in $\{0.1, 0.3, 0.5, 0.7, 0.9\}(\pm 0.1)$ we generated 20 random seeds of length 50. For each seed, at each mutational distance (i.e. number of mutations from the seed) from 0 to 50, at least 10 000 sequence-structure pairs within the target GC content of the seed were sampled from the Boltzmann distribution. The software was run on Dual Intel Westmere EP Xeon X5650 (6-core, 2.66 GHz, 12MB Cache, 95W) on the Guillimin High Performance Computing Cluster of Calcul Québec. It took over 12 000 CPU hours to complete the sampling.

4.2.1 Sequence-structure pairs weighted sampling

Given a seed sequence ω_0, a fixed number of mutations k, and the ensemble $\mathbb{S}^k_{\omega_0}$ of all pairs sequence-structure such that the sequences are at hamming k from ω_0. Similarly to Sec. 4.1.2 the *fitness* of a sequence-structure pair $(\omega, s) \in \mathbb{S}^k_{\omega_0}$ will be its Boltzmann weight, a function of its energy.

Formally, if the energy of the sequence ω in conformation s is $E(\omega, s)$ then the weight of the pair is:

$$e^{\frac{-E(\omega,s)}{RT}}$$

where as before the Boltzmann constant R equals $0.000\,198\,71$ kcal mol^{-1} K^{-1}and the temperature T is set at $310.15K$. The normalization factor, or partition function, $\mathcal{Z}$ can now be defined as:

$$\mathcal{Z} = \sum_{(\omega',s')\in\mathbb{S}^k_{\omega_0}} e^{\frac{-E(\omega',s')}{RT}}$$

and thus the probability of sampling a pair (ω, s) is:

$$\mathbb{P}(\omega, s) = \frac{e^{\frac{-E(\omega,s)}{RT}}}{\mathcal{Z}}.$$

By increasing k from 1 to $|\omega_0|$ an exploration of whole mutational landscape of ω_0 is performed. To compute $\mathcal{Z}$ for each value of k, `RNAmutants` has a complexity of $\mathcal{O}(n^3k^2)$. This has to be done only once per seed. The weighted sampling of the sequences themselves has complexity of $\mathcal{O}(n^2)$.

4.2.2 Controlling sample GC content

Due to the deep correlation between the GC content of the sequence and its energy, the GC base pair being the most energetic in the Turner model [67] which is used by `RNAmutants`, sampling from any ensemble $\mathbb{S}$ will be highly biased towards sequences with high GC content. To get a sample (ω, s) at a specific target GC content, a natural approach is to continuously sample and reject any sequence not fitting the requirements. Such an approach can yield an exponential time so a technique developed in [49] is applied.

An unbiased sampling of pairs (ω, s) for any given GC target can be obtained by modifying the Boltzmann weights of any element (ω, s) with a term $\mathbf{w}^\omega \in [0, 1]$ which depends on the GC content of ω. At its simplest, it can be the proportion of GC in ω. The weight of (ω, s) becomes

$$\mathbf{w}^\omega e^{\frac{-E(\omega,s)}{RT}}$$

which implies that a new partition function $\mathcal{Z}^{\mathbf{w}}$ needs to be defined as follows:

$$\mathcal{Z}^{\mathbf{w}} = \sum_{(\omega',s')\in\mathbb{S}^k_{\omega_0}} \mathbf{w}^{\omega} e^{\frac{-E(\omega',s')}{RT}}.$$

To find the weights $\mathbf{w}$ for any target GC an exact solution could be found. In practice, the weight $\mathbf{w}^{\omega}$ is determined as follows, applying the bissection algorithm. Given the number of GC in ω, $|\omega|_{\mathrm{GC}}$ (resp number of AU $|\omega|_{\mathrm{AU}}$) and two weight $\mathbf{w}_{\mathrm{GC}}$ and $\mathbf{w}_{\mathrm{AU}}$. We define $\mathbf{w}^{\omega}$ as $\mathbf{w}^{\omega} := \mathbf{w}_{\mathrm{GC}}^{|\omega|_{\mathrm{GC}}} \times \mathbf{w}_{\mathrm{AU}}^{|\omega|_{\mathrm{AU}}}$. At the first iteration, a thousand sequences are sampled with $\mathbf{w}_{\mathrm{GC}}$ and $\mathbf{w}_{\mathrm{AU}}$ both as 0.5. If the average GC content on the sampled sequences is too high, the value of $\mathbf{w}_{\mathrm{GC}}$ is decreased by half and $\mathbf{w}_{\mathrm{AU}}$ increased accordingly. If the average GC content is too low, the opposite is done. Each time, the sequences with the desired GC content are kept. This process is repeated until the desired amount of sequences with the required GC content is produced. In practice, after a few iterations almost all sampled sequences contain the target GC content and as shown this sampling is unbiased [49]. An interesting observation is that the same method can be applied to preferentially sample sequences with any other desired feature.

4.3 Sequence divergence in an random replication model

We estimate the expected number of mutations in randomly replicated sequences (section 2.3) using the transition matrix defined by K. Tamura [55]. We use a mutation rate $\alpha = 0.02$ mirroring the mutation rate used in `mateRNAl`, and assume that transition and transversion rates are identical. The target GC content is represented with the variable $\theta = \{0.1, 0.3, 0.5, 0.7, 0.9\}$. The transition matrix is shown below.

	A	U	C	G
A	$1-\alpha(1+\theta)$	$(1-\theta)\alpha$	$\theta\alpha$	$\theta\alpha$
U	$(1-\theta)\alpha$	$1-\alpha(1+\theta)$	$\theta\alpha$	$\theta\alpha$
C	$(1-\theta)\alpha$	$(1-\theta)\alpha$	$1-(1-\alpha(1+\theta))$	$\theta\alpha$
G	$(1-\theta)\alpha$	$(1-\theta)\alpha$	$\theta\alpha$	$1-(1-\alpha(1+\theta))$

This matrix gives us the transition rate from one generation to the next one. To obtain the mutation probabilities at the kth generation, we calculate the kth exponent of this matrix. Then, we sum the values along the main diagonal to estimate the probability of a nucleotide to be the same at the initial and k^{th} generation.

5 Author contributions

CGO, VR, and JW designed the research, analyzed the results, and wrote the manuscript. CO and VR conducted the computational experiments.

6 Funding

CGO is supported by a Fonds de Recherche Nature et Technologie Quebec (FRQNT) Doctoral Fellowship. VR is supported by a Fonds de Recherche Nature et Technologie Quebec (FRQNT) and Azrieli Postdoctoral Fellowships. JW is supported by a NSERC Discovery grant (RGPIN-2015-03786), NSERC Accelerator Award (RGPAS 477873-15), and FRQ-NT INRIA associated teams (211485).

References

[1] Walter Gilbert. Origin of life: The RNA world. *Nature*, 319:618, February 1986. doi: 10.1038/319618a0.

[2] S R Eddy. Non-coding RNA genes and the modern RNA world. *Nat Rev Genet*, 2(12):919–29, Dec 2001. doi: 10.1038/35103511.

[3] Robert Shapiro. A simpler origin for life. *Scientific American*, 296(6):46–53, 2007. ISSN 00368733, 19467087. URL `http://www.jstor.org/stable/26069306`.

[4] Leslie E Orgel. Prebiotic chemistry and the origin of the rna world. *Crit Rev Biochem Mol Biol*, 39(2):99–123, 2004. doi: 10.1080/10409230490460765.

[5] Michael P Robertson and Gerald F Joyce. The origins of the rna world. *Cold Spring Harb Perspect Biol*, 4(5), May 2012. doi: 10.1101/cshperspect.a003608.

[6] Matthew W Powner, Béatrice Gerland, and John D Sutherland. Synthesis of activated pyrimidine ribonucleotides in prebiotically plausible conditions. *Nature*, 459(7244):239–42, May 2009. doi: 10.1038/nature08013.

[7] Dougal Ritson and John D Sutherland. Prebiotic synthesis of simple sugars by photoredox systems chemistry. *Nat Chem*, 4(11):895–9, Nov 2012. doi: 10.1038/nchem.1467.

[8] David P Horning and Gerald F Joyce. Amplification of RNA by an RNA polymerase ribozyme. *Proc Natl Acad Sci U S A*, 113(35):9786–91, Aug 2016. doi: 10.1073/pnas.1610103113.

[9] Sidney Becker, Ines Thoma, Amrei Deutsch, Tim Gehrke, Peter Mayer, Hendrik Zipse, and Thomas Carell. A high-yielding, strictly regioselective prebiotic purine nucleoside formation pathway. *Science*, 352(6287):833–6, May 2016. doi: 10.1126/science.aad2808.

[10] Ben K D Pearce, Ralph E Pudritz, Dmitry A Semenov, and Thomas K Henning. Origin of the rna world: The fate of nucleobases in warm little ponds. *Proc Natl Acad Sci U S A*, 114 (43):11327–11332, 10 2017. doi: 10.1073/pnas.1710339114.

[11] Jack W. Szostak. The eightfold path to non-enzymatic rna replication. *Journal of Systems Chemistry*, 3(1):2, Feb 2012. ISSN 1759-2208. doi: 10.1186/1759-2208-3-2. URL `https://doi.org/10.1186/1759-2208-3-2`.

[12] Eric P Nawrocki, Sarah W Burge, Alex Bateman, Jennifer Daub, Ruth Y Eberhardt, Sean R Eddy, Evan W Floden, Paul P Gardner, Thomas A Jones, John Tate, and Robert D Finn. Rfam 12.0: updates to the RNA families database. *Nucleic Acids Res*, 43(Database issue): D130–7, Jan 2015. doi: 10.1093/nar/gku1063.

[13] Paul G Higgs and Niles Lehman. The RNA World: molecular cooperation at the origins of life. *Nat Rev Genet*, 16(1):7–17, Jan 2015. doi: 10.1038/nrg3841.

[14] C Reidys, P F Stadler, and P Schuster. Generic properties of combinatory maps: neutral networks of RNA secondary structures. *Bull Math Biol*, 59(2):339–97, Mar 1997.

[15] Ronny Lorenz, Stephan H Bernhart, Christian Höner Zu Siederdissen, Hakim Tafer, Christoph Flamm, Peter F Stadler, and Ivo L Hofacker. ViennaRNA package 2.0. *Algorithms Mol Biol*, 6:26, 2011. doi: 10.1186/1748-7188-6-26.

[16] Walter Fontana, Thomas Griesmacher, Wolfgang Schnabl, Peter F Stadler, and Peter Schuster. Statistics of landscapes based on free energies, replication and degradation rate constants

of RNA secondary structures. *Monatshefte für Chemie/Chemical Monthly*, 122(10):795–819, 1991.

[17] Peter Schuster and Peter F Stadler. Landscapes: Complex optimization problems and biopolymer structures. *Computers & chemistry*, 18(3):295–324, 1994.

[18] Walter Gruner, Robert Giegerich, Dirk Strothmann, Christian Reidys, Jacqueline Weber, Ivo L Hofacker, Peter F Stadler, Peter Schuster, et al. Analysis of RNA sequence structure maps by exhaustive enumeration. *Monatsh Chem*, 127(355), 1996.

[19] Peter Schuster and Walter Fontana. Chance and necessity in evolution: lessons from RNA. *Physica D: Nonlinear Phenomena*, 133(1-4):427–452, September 1999. ISSN 01672789. doi: 10.1016/S0167-2789(99)00076-7. URL `http://linkinghub.elsevier.com/retrieve/pii/S0167278999000767`.

[20] Peter Schuster. Evolution in silico and in vitro: the RNA model. *Biological chemistry*, 382(9): 1301–1314, 2001.

[21] E van Nimwegen, J P Crutchfield, and M Huynen. Neutral evolution of mutational robustness. *Proc Natl Acad Sci U S A*, 96(17):9716–20, Aug 1999.

[22] L W Ancel and W Fontana. Plasticity, evolvability, and modularity in RNA. *J Exp Zool*, 288 (3):242–83, Oct 2000.

[23] C O Wilke. Selection for fitness versus selection for robustness in RNA secondary structure folding. *Evolution; international journal of organic evolution*, 55(12):2412–20, December 2001. ISSN 0014-3820. URL `http://www.ncbi.nlm.nih.gov/pubmed/11831657`.

[24] Jacobo Aguirre, Javier M Buldú, Michael Stich, and Susanna C Manrubia. Topological structure of the space of phenotypes: the case of RNA neutral networks. *PLoS One*, 6(10):e26324, 2011. doi: 10.1371/journal.pone.0026324.

[25] Kamaludin Dingle, Steffen Schaper, and Ard A Louis. The structure of the genotype-phenotype map strongly constrains the evolution of non-coding RNA. *Interface Focus*, 5(6):20150053, Dec 2015. doi: 10.1098/rsfs.2015.0053.

[26] Anne Kupczok and Peter Dittrich. Determinants of simulated RNA evolution. *Journal of theoretical biology*, 238(3):726–35, February 2006. ISSN 0022-5193. doi: 10.1016/j.jtbi.2005.06.019. URL `http://www.ncbi.nlm.nih.gov/pubmed/16098538`.

[27] Michael Stich, Carlos Briones, and Susanna C Manrubia. Collective properties of evolving molecular quasispecies. *BMC evolutionary biology*, 7:110, January 2007. ISSN 1471-2148. doi: 10.1186/1471-2148-7-110. URL `http://www.pubmedcentral.nih.gov/articlerender.fcgi?artid=1934359\&tool=pmcentrez\&rendertype=abstract`.

[28] Michael Stich, Susanna C Manrubia, and Ester La. Variable Mutation Rates as an Adaptive Strategy in Replicator Populations. *PLoS ONE*, 5(6), 2010. doi: 10.1371/Citation.

[29] Michael Stich, Carlos Briones, and Susanna C Manrubia. On the structural repertoire of pools of short, random RNA sequences. *Journal of theoretical biology*, 252(4):750–763, 2008.

[30] P Schuster, W Fontana, P F Stadler, and I L Hofacker. From sequences to shapes and back: a case study in RNA secondary structures. *Proc Biol Sci*, 255(1344):279–84, Mar 1994. doi: 10.1098/rspb.1994.0040.

[31] W Fontana and P Schuster. Shaping space: the possible and the attainable in RNA genotype-phenotype mapping. *J Theor Biol*, 194(4):491–515, Oct 1998. doi: 10.1006/jtbi.1998.0771.

[32] M Levy and A D Ellington. The descent of polymerization. *Nat Struct Biol*, 8(7):580–2, Jul 2001. doi: 10.1038/89601.

[33] Eric J Hayden and Niles Lehman. Self-assembly of a group I intron from inactive oligonucleotide fragments. *Chem Biol*, 13(8):909–18, Aug 2006. doi: 10.1016/j.chembiol.2006.06.014.

[34] Nilesh Vaidya, Michael L Manapat, Irene A Chen, Ramon Xulvi-Brunet, Eric J Hayden, and Niles Lehman. Spontaneous network formation among cooperative RNA replicators. *Nature*, 491(7422):72–7, Nov 2012. doi: 10.1038/nature11549.

[35] A A Beaudry and G F Joyce. Directed evolution of an RNA enzyme. *Science*, 257(5070):635–41, Jul 1992.

[36] D P Bartel and J W Szostak. Isolation of new ribozymes from a large pool of random sequences. *Science*, 261(5127):1411–8, Sep 1993.

[37] Erik A Schultes, Alexander Spasic, Udayan Mohanty, and David P Bartel. Compact and ordered collapse of randomly generated RNA sequences. *Nat Struct Mol Biol*, 12(12):1130–6, Dec 2005. doi: 10.1038/nsmb1014.

[38] Abe Pressman, Janina E. Moretti, Gregory W. Campbell, Ulrich F. Müller, and Irene A. Chen. Analysis of in vitro evolution reveals the underlying distribution of catalytic activity among random sequences. *Nucleic Acids Research*, 45(14):8167–8179, 2017. doi: 10.1093/nar/gkx540.

[39] K Salehi-Ashtiani and J W Szostak. In vitro evolution suggests multiple origins for the hammerhead ribozyme. *Nature*, 414(6859):82–4, Nov 2001. doi: 10.1038/35102081.

[40] Péter Szabó, István Scheuring, Tamás Czárán, and Eörs Szathmáry. In silico simulations reveal that replicators with limited dispersal evolve towards higher efficiency and fidelity. *Nature*, 420(6913):340–3, Nov 2002. doi: 10.1038/nature01187.

[41] Carlos Briones, Michael Stich, and Susanna C Manrubia. The dawn of the RNA World: toward functional complexity through ligation of random RNA oligomers. *RNA*, 15(5):743–9, May 2009. doi: 10.1261/rna.1488609.

[42] Julie A Shay, Christopher Huynh, and Paul G Higgs. The origin and spread of a cooperative replicase in a prebiotic chemical system. *J Theor Biol*, 364:249–59, Jan 2015. doi: 10.1016/j.jtbi.2014.09.019.

[43] Nikola A Ivica, Benedikt Obermayer, Gregory W Campbell, Sudha Rajamani, Ulrich Gerland, and Irene A Chen. The paradox of dual roles in the RNA world: resolving the conflict between stable folding and templating ability. *Journal of molecular evolution*, 77(3):55–63, 2013.

[44] Irene A Chen, Kourosh Salehi-Ashtiani, and Jack W Szostak. Rna catalysis in model protocell vesicles. *J Am Chem Soc*, 127(38):13213–9, Sep 2005. doi: 10.1021/ja051784p.

[45] Katarzyna Adamala and Jack W Szostak. Nonenzymatic template-directed rna synthesis inside model protocells. *Science*, 342(6162):1098–100, Nov 2013. doi: 10.1126/science.1241888.

[46] Derek K O'Flaherty, Neha P Kamat, Fatima N Mirza, Li Li, Noam Prywes, and Jack W Szostak. Copying of mixed-sequence rna templates inside model protocells. *J Am Chem Soc*, 140(15):5171–5178, 04 2018. doi: 10.1021/jacs.8b00639.

[47] Peter Schuster. Prediction of rna secondary structures: from theory to models and real molecules. *Reports on Progress in Physics*, 69(5):1419, 2006.

[48] Jérôme Waldispühl, Srinivas Devadas, Bonnie Berger, and Peter Clote. Efficient algorithms for probing the RNA mutation landscape. *PLoS Comput Biol*, 4(8):e1000124, Aug 2008. doi: 10.1371/journal.pcbi.1000124.

[49] Jérôme Waldispühl and Yann Ponty. An unbiased adaptive sampling algorithm for the exploration of RNA mutational landscapes under evolutionary pressure. *Journal of Computational Biology*, 18(11):1465–1479, 2011.

[50] Matthew C Cowperthwaite, Evan P Economo, William R Harcombe, Eric L Miller, and Lauren Ancel Meyers. The ascent of the abundant: how mutational networks constrain evolution. *PLoS Comput Biol*, 4(7):e1000110, Jul 2008. doi: 10.1371/journal.pcbi.1000110.

[51] Kevin Leu, Benedikt Obermayer, Sudha Rajamani, Ulrich Gerland, and Irene A Chen. The prebiotic evolutionary advantage of transferring genetic information from RNA to DNA. *Nucleic Acids Res*, 39(18):8135–47, Oct 2011. doi: 10.1093/nar/gkr525.

[52] David Penny and Anthony Poole. The nature of the last universal common ancestor. *Current opinion in genetics & development*, 9(6):672–677, 1999.

[53] Paul P Gardner, Barbara R Holland, Vincent Moulton, Mike Hendy, and David Penny. Optimal alphabets for an RNA world. *Proc Biol Sci*, 270(1520):1177–82, Jun 2003. doi: 10.1098/rspb.2003.2355.

[54] Adrian R Ferré-D'Amaré and William G Scott. Small self-cleaving ribozymes. *Cold Spring Harb Perspect Biol*, 2(10):a003574, Oct 2010. doi: 10.1101/cshperspect.a003574.

[55] K Tamura. Estimation of the number of nucleotide substitutions when there are strong transition-transversion and G+C-content biases. *Mol Biol Evol*, 9(4):678–87, Jul 1992.

[56] Alex Levin, Mieszko Lis, Yann Ponty, Charles W O'Donnell, Srinivas Devadas, Bonnie Berger, and Jérôme Waldispühl. A global sampling approach to designing and reengineering RNA secondary structures. *Nucleic Acids Res*, 40(20):10041–52, Nov 2012. doi: 10.1093/nar/gks768.

[57] Ryan Kennedy, Manuel E Lladser, Zhiyuan Wu, Chen Zhang, Michael Yarus, Hans De Sterck, and Rob Knight. Natural and artificial RNAs occupy the same restricted region of sequence space. *RNA*, 16(2):280–9, Feb 2010. doi: 10.1261/rna.1923210.

[58] Sandra Smit, Michael Yarus, and Rob Knight. Natural selection is not required to explain universal compositional patterns in rRNA secondary structure categories. *RNA*, 12(1):1–14, Jan 2006. doi: 10.1261/rna.2183806.

[59] S F Greenbury and S E Ahnert. The organization of biological sequences into constrained and unconstrained parts determines fundamental properties of genotype-phenotype maps. *J R Soc Interface*, 12(113):20150724, Dec 2015. doi: 10.1098/rsif.2015.0724.

[60] Susanna Manrubia and José A Cuesta. Distribution of genotype network sizes in sequence-to-structure genotype-phenotype maps. *J R Soc Interface*, 14(129), Apr 2017. doi: 10.1098/rsif.2016.0976.

[61] Robert Pascal, Addy Pross, and John D Sutherland. Towards an evolutionary theory of the origin of life based on kinetics and thermodynamics. *Open Biol*, 3(11):130156, Nov 2013. doi: 10.1098/rsob.130156.

[62] A R Hill, Jr, L E Orgel, and T Wu. The limits of template-directed synthesis with nucleoside-5'-phosphoro(2-methyl)imidazolides. *Orig Life Evol Biosph*, 23(5-6):285–90, Dec 1993.

[63] J Waldispühl, B Behzadi, and J-M Steyaert. An approximate matching algorithm for finding (sub-)optimal sequences in S-attributed grammars. *Bioinformatics*, 18 Suppl 2:S250–9, 2002.

[64] Susanna C Manrubia and Carlos Briones. Modular evolution and increase of functional complexity in replicating RNA molecules. *RNA*, 13(1):97–107, 2007.

[65] Sudha Rajamani, Justin K Ichida, Tibor Antal, Douglas A Treco, Kevin Leu, Martin A Nowak, Jack W Szostak, and Irene A Chen. Effect of stalling after mismatches on the error catastrophe

in nonenzymatic nucleic acid replication. *J Am Chem Soc*, 132(16):5880–5, Apr 2010. doi: 10.1021/ja100780p.

[66] Eörs Szathmáry. The origin of replicators and reproducers. *Philos Trans R Soc Lond B Biol Sci*, 361(1474):1761–76, Oct 2006. doi: 10.1098/rstb.2006.1912.

[67] Douglas H Turner and David H Mathews. NNDB: the nearest neighbor parameter database for predicting stability of nucleic acid secondary structure. *Nucleic acids research*, page gkp892, 2009.

[68] Kévin Darty, Alain Denise, and Yann Ponty. Varna: Interactive drawing and editing of the rna secondary structure. *Bioinformatics*, page btp250, 2009.

Figures

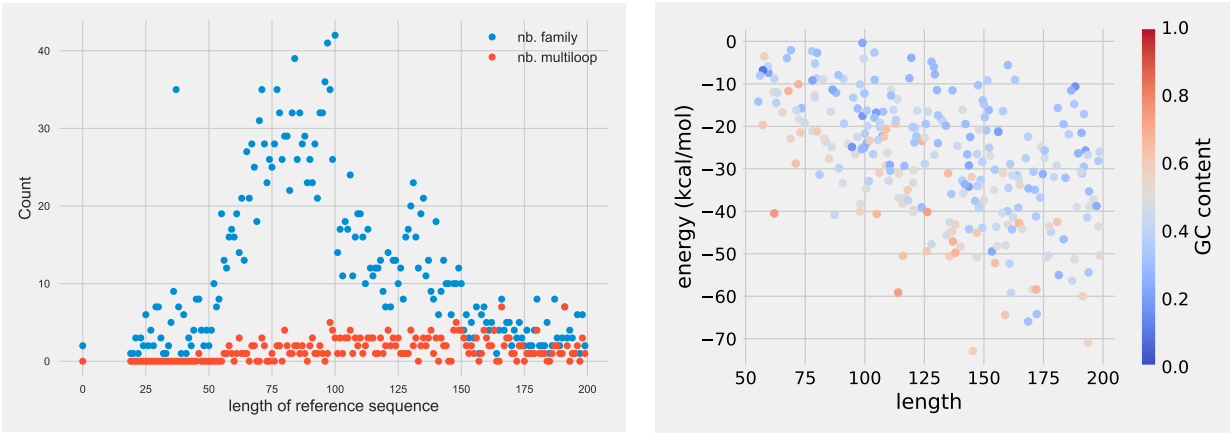

(a) (b)

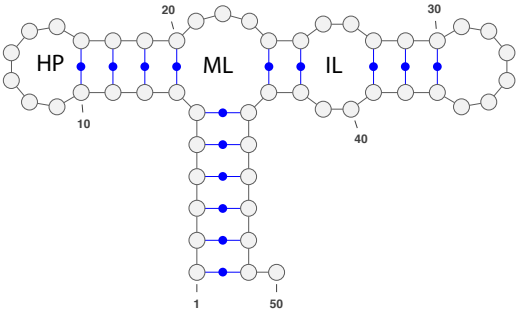

(c)

Figure 1: Statistics on Rfam families [12]. On the left, the graph plots the number of families with respect to the average length of the sequences in these families. Red dots show the numbers of families with a consensus structure that contains a multi-loop, while blue dots show those without. On the right, we plot the average folding energy and length of sequences for each Rfam families having multi-branched consensus structures. The color indicates the average GC content of the family. On the bottom we show an illustration of an RNA 2D fold (generated using VARNA [68]) and label its secondary structure elements as internal loop (IL), multi-loop (ML) and hairpin (HP).

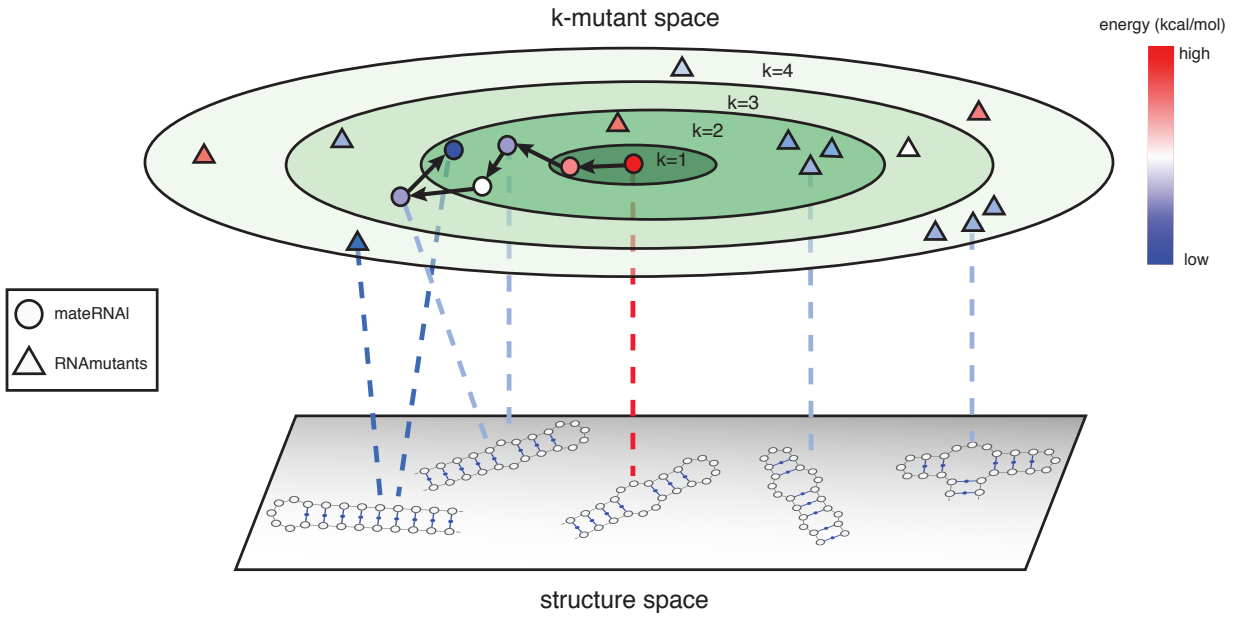

Figure 2: *Illustration of mutational sampling methods.* Concentric ellipses represent the space of sequence k-mutant neighbourhoods around a root sequence pictured at the centre of the ellipses. Each ring holds all sequences that are k mutations from the root. We show the contrast between an evolutionary trajectory (`mateRNAl`) along this space and mutational ensemble sampling (`RNAmutants`) represented respectively as circles and triangles. The layer below the mutational space represents the space of all possible secondary structures, and dotted lines illustrate the mapping from sequences to structures. The colour of the sampled mutants denotes the energy of the sequence-structure pair sampled. In both sampling methods, sequence-structure pairs with lower energies are favoured. Evolutionary sampling is always limited to explore sequences accessible from the parental sequence and so we have arrows pointing from parents to children over various generations yielding an adaptive trajectory. `RNAmutants` considers the entire ensemble of k mutants to generate independent samples of stable sequence-structure pairs and thus reveals features such as complex structures that are hard to reach by local methods such as `mateRNAl`.

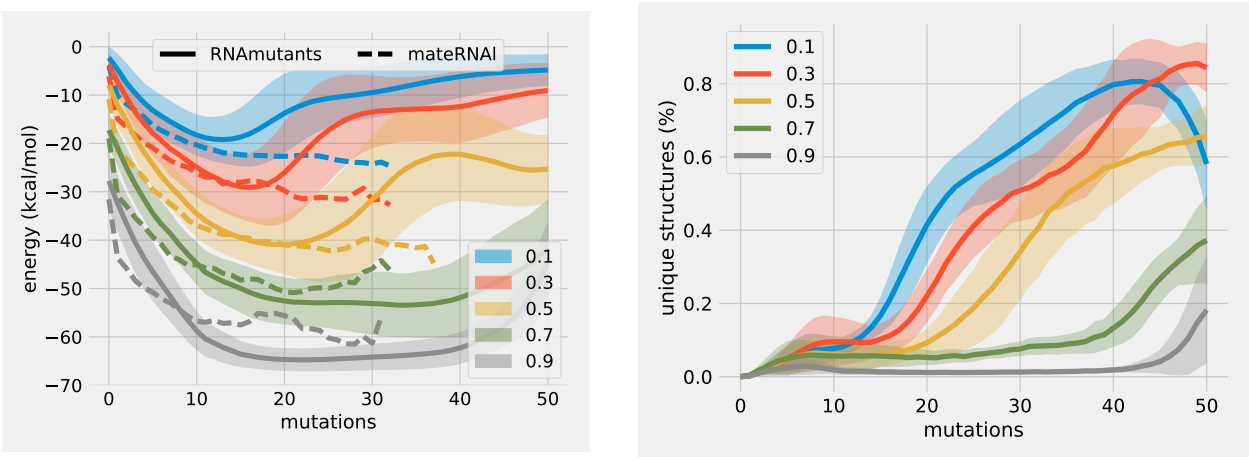

(a) (b)

Figure 3: (a) Energy of `RNAmutants` and `mateRNAl` mutational landscape. Shaded regions include one standard deviation of `RNAmutants` energy per mutational distance. Dashed lines mark mean values for `mateRNAl` energies binned by mutations from starting sequence using mutation rate $\mu = 0.02$. (b) Fraction of unique structures at every k neighbourhood found by `RNAmutants`.

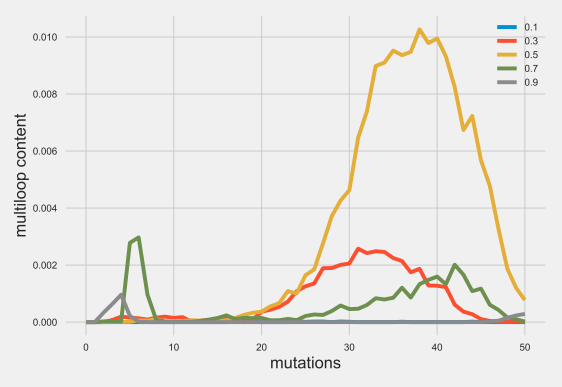

(a) Frequency vs mutational distance

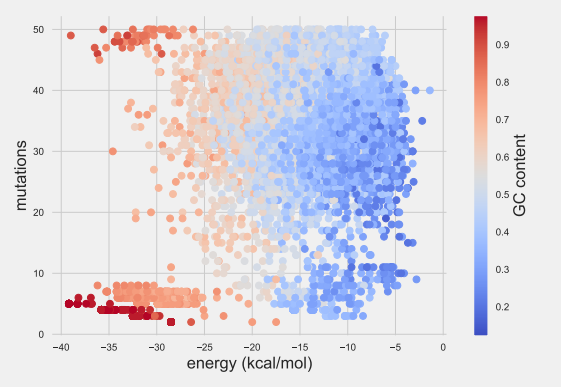

(b) multi-loop energy map

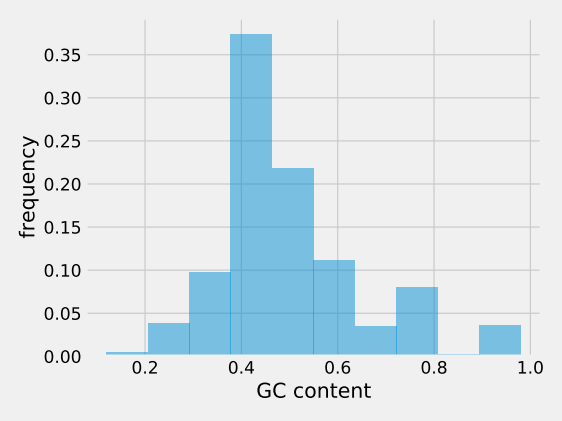

(c) GC content distribution

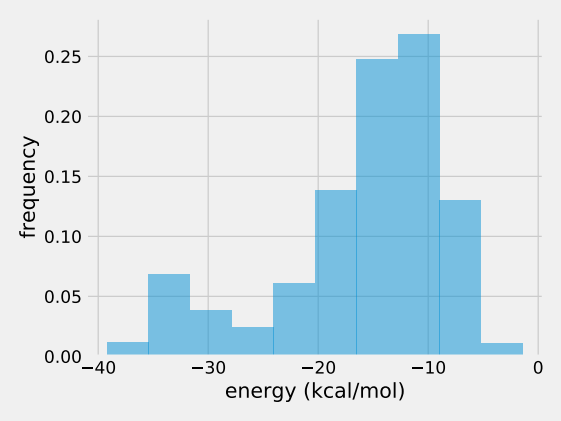

(d) Energy distribution

Figure 4: Analysis of the distribution of multi-branched structures in the RNA mutational landscape sampled by `RNAmutants`. (a) The frequency of multi-branched structures with respect to the number of mutations from the seed sequence. (b) Plot of folding energies and GC contents of each individual multi-branched structure. (c) Distribution of the GC content of multi-branched structures. (d) Distribution of folding energies of multi-branched structures.

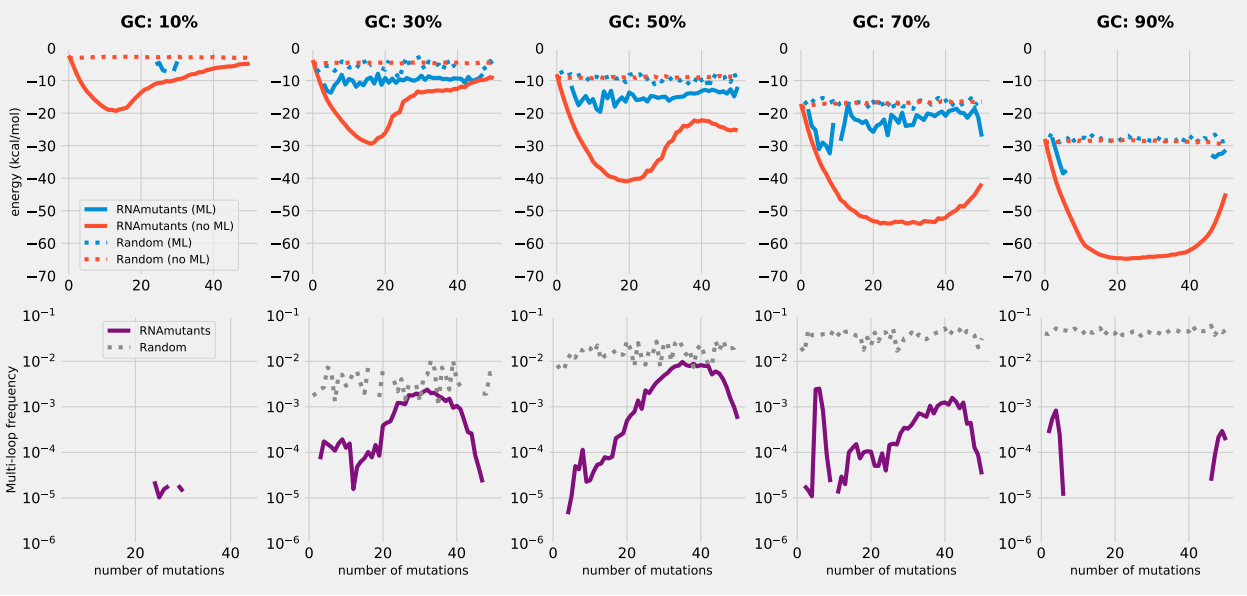

Figure 5: Analysis of multi-loop distributions in uniform and low energy populations. First row: average minimum free energies of uniformly sampled mutants ("Random"; dotted lines) and sequences from the low energy ensemble ("RNAmutants"; plain lines). Sequences with a minimum free energy structure having a multi-loop ("ML"; blue) are separated from the others ("no ML"; orange). Second row: frequency of multi-branched structures in the minimum free energy structure of uniformly sampled mutants ("Random"; dotted grey lines) and sequences sampled from the low energy ensemble ("RNAmutants"; purple lines)

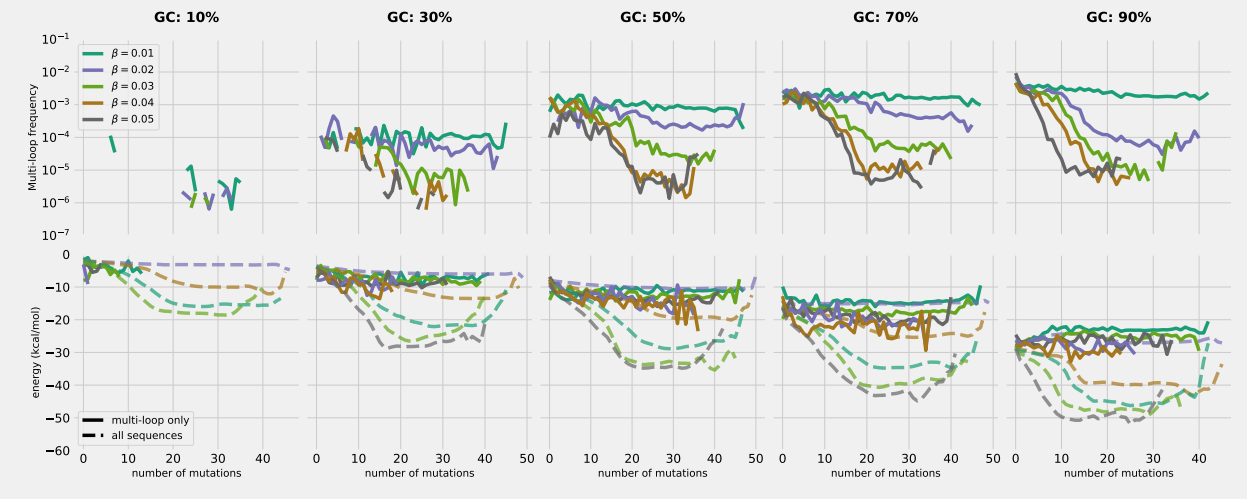

Figure 6: Analysis of multi-loop frequency and energy in `mateRNA1` populations as a function of mutational distance. First row: average frequency of multiloop structures in populations at each mutational distance. Each line represents a simulation at varying selection strengths (parameter β). Subplot columns correspond to simulations at various GC content biases. Second row: Average population energy at each mutational distance. Plain lines report statistics calculated for multi-branched structures only, while dashed lines show the measurements obtained for all structures.

Supplemental Materials: "The necessary emergence of structural complexity in self-replicating RNA populations"

Carlos Oliver, Vladimir Reinharz, Jérôme Waldispühl

1 Sampling schemes

`RNAmutants` samples sequence-structure pairs according to their ensemble weight. This method therefore does not guarantee the sampling of the minimum free energy (MFE) structure for a given sequence. However, for a given "suboptimal" sampling we can use `RNAfold` to obtain the MFE structure for every sequence, producing a set of sequence-structure pairs that can be directly compared to `mateRNAl` data which samples only MFE structures. In **Fig. S1** we show that this procedure produces sequence-structure pairs with nearly identical ensemble frequencies, allowing us to proceed with MFE structures in downstream analysis.

2 Energy landscapes

With free energy being the driving force in our simulations, we next compared mean energy values for mutation populations in `mateRNAl` and `RNAmutants`. We show in **Fig. S2** that a random starting seed in `RNAmutants` is on average under 15 mutations away from the global minimum of its mutational ensemble. This feature of the energy of mutational landscapes is exploited by the local search nature of `mateRNAl` which is able to rapidly identify stable solutions with very few mutations. More specifically, we tested various mutation rates (μ) for `mateRNAl` and superimposed mean values to those obtained by `RNAmutants`, **Fig. S3**. We note that higher mutation rates lead to deeper mutational explorations yet never reaching as far as `RNAmutants`. Regardless, it appears that the most stable structures are maintained at lower mutation rates, suggesting a tradeoff between exploration and refinement.

3 Structural complexity

Here we summarize the structural features discovered by `mateRNAl` and `RNAmutants`. In this study we distinguish between three major structural features: stack, internal loop, and multiloop. The

stack is produced from consecutive base pairing interactions and thus higher stack numbers form longer stem structures. These represent the simplest of the structural motifs. The internal loop occurs when a stacking is interrupted by unpaired bases forming a loop like structure within a stem. A multi-loop is also an unpaired region that forms a loop but which connects three or more stems, also known as a junction. **Fig. S4** shows the effect of GC content on the occurence of internal looping structures as a function of mutational distance in `RNAmutants` simulations.

4 Analysis of Hamming neighbourhoods

We provide complementary data to characterize the sequences available at specific mutational distances and GC contents. **Fig. S5** shows the number of mutations accumulated in populations evolving under a random model preserving the GC content. We use for this purpose the model introduced by K. Tamura [55] (See Sec. 4.3). **Fig. S6** indicates the number of sequences with exactly k mutations and with a GC content within ± 0.1 of the target GC content. Thus, it shows the size of the neighbourhoods.

Figures

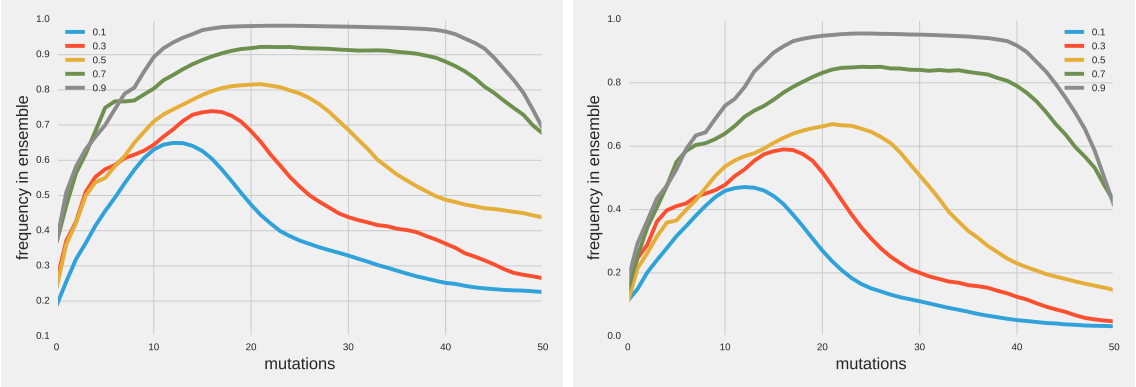

(a) MFE

(b) Sampled

Figure S1: Frequency of sequence-structure pair in Boltzmann ensemble for MFE and suboptimal sampling in RNAmutants.

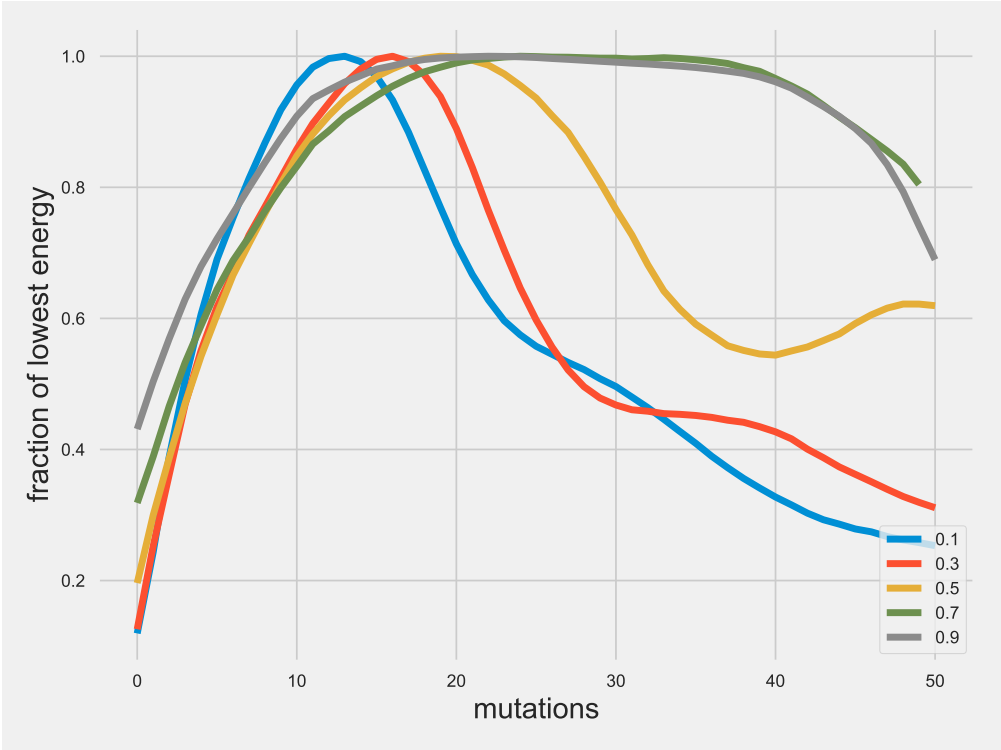

Figure S2: Percentage of the global minimum energy reached by RNAmutants by mutational distance.

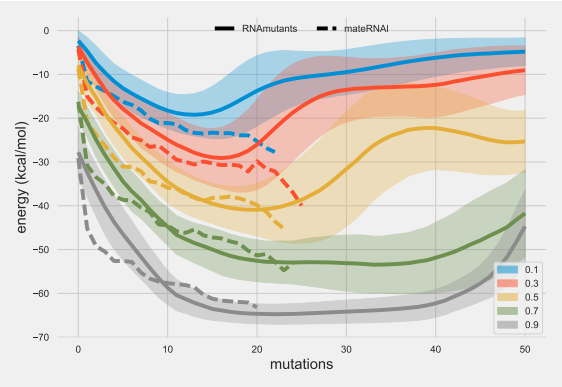

(a) $\mu = 0.001$

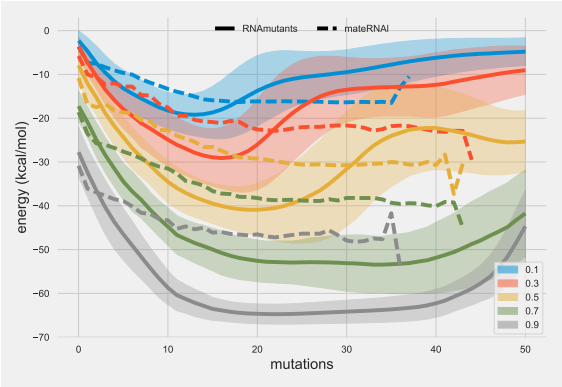

(b) $\mu = 0.1$

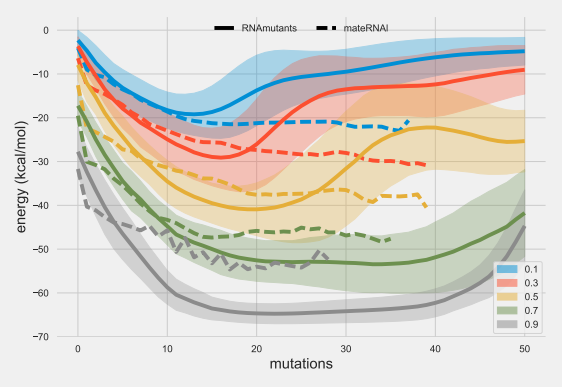

(c) $\mu = 0.05$

Figure S3: Average energy comparison between `mateRNAl` and `RNAmutants` using different mutation rates for `mateRNAl`.

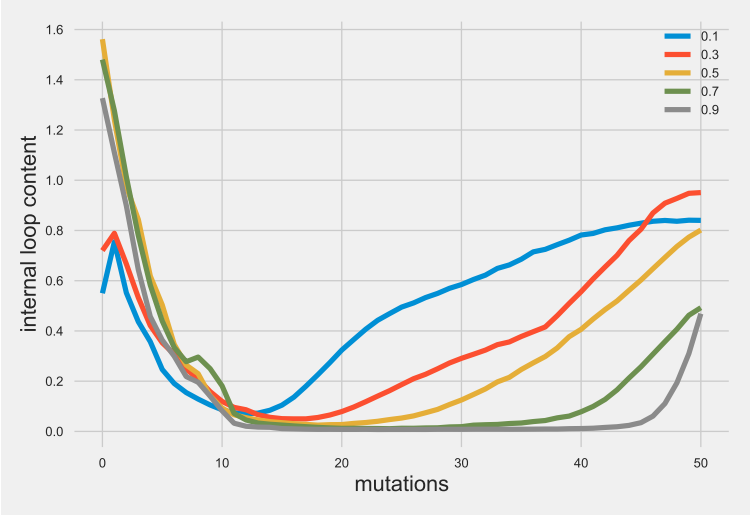

Figure S4: Fraction of k-mutant neighbourhoods populated with internal looping structures in `RNAmutants`.

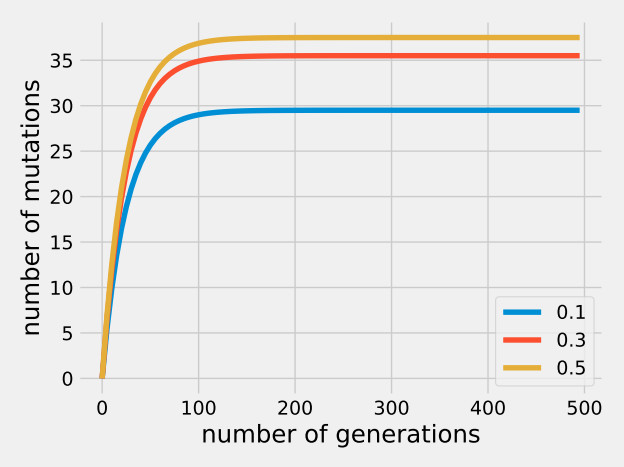

Figure S5: Number of mutations accumulated in populations evolving under a random GC-preserving replication model.

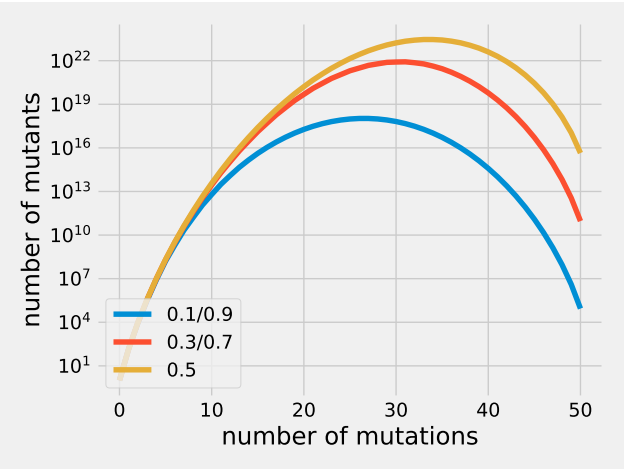

Figure S6: Number of sequences in hamming neighbourhoods.